Hardware Testing For Error Tolerant Multimedia Compression based on Linear Transforms [*]

In Suk Chong and Antonio Ortega

Signal and Image Processing Institute
Department of Electrical Engineering-Systems,
University of Southern California,
Los Angeles CA 90089-2563
ichong@usc.edu, ortega@sipi.usc.edu

Abstract

In this paper, we propose a system-level error tolerance scheme for systems where a linear transform is combined with quantization. These are key components in multimedia compression systems, e.g., video and image codecs. Using the concept of acceptable degradation, our scheme classifies hardware faults into acceptable and unacceptable faults. We propose analysis techniques that allow us to estimate the faults' impact on compression performance, and in particular on the quality of decoded images/video. We consider as an example the Discrete Cosine Transform (DCT), which is part of a large number of existing image and video compression systems. We propose methods to establish thresholds of acceptable degradation and corresponding testing algorithms for DCT-based systems. Our results for a JPEG encoder using a typical DCT architecture show that over 50% of single stuck-at interconnection faults in one of its 1D DCT modules lead to imperceptible quality degradation in the decoded images, over the complete range of compression rates at which JPEG can operate.

1. Introduction

Classical manufacturing test for digital chips classifies chips into two categories: perfect and imperfect. Our work is motivated by the notion that in some instances imperfect chips can be used, as long as they introduce "acceptable errors". Error tolerance (ET) leads to a relaxation of the requirement of 100% correctness for devices and interconnects, which may dramatically reduce costs for manufacturing, verification, and testing [4]. Categorizing chips into acceptable and unacceptable also leads to increases in yield rate.

Determining what constitutes acceptable degradation in system performance is obviously an application-specific decision; both performance criteria and acceptability thresholds are highly dependent on the application. In this paper we consider multimedia compression systems as a promising application area for our proposed ET concepts. This is because i) many multimedia compression systems are deployed in consumer devices, for which maintaining low costs is important, and ii) compression itself leads to a lossy representation of signals, so that the effect of system faults can be viewed as an additional source of "noise" or representation error. As an example, our study of a complete MPEG video encoder [5] indicates that several of its building blocks, in particular its Motion Estimation (ME) component, are such that some hardware faults lead to acceptable degradation at the system outputs [5, 6].

In this paper we focus on a very common component of multimedia compression systems, namely the discrete cosine transform (DCT). This transform is used in video coders, e.g., MPEG [9], and image coders,

e.g., JPEG [8], and similar linear block transforms are used in emerging compression systems, such as ITU-T H.264 [2]. Note that in all these systems the transform is followed by quantization. Thus, while we consider faults in the transform operation, our analysis considers the impact of the faults *after* quantization.

To provide some intuition about the impact of faults in the DCT, consider Table 1, where we show the average peak signal to noise ratio (PSNR) degradation produced by single stuck-at faults (SSF) at the input of a DCT block. PSNR is a well acccepted objective quality metric used in image/video compression. Note that some faults generate acceptable degradation. For example, if we set the acceptable PSNR degradation to be less than $0.2dB$, we see that more than half the faults at the input are acceptable[1]. Observe also from Table 1 that a fault's impact depends on the choice of quantization parameters, so that, as expected, a given fault in the transform computation will tend to have a lesser impact as the quantization becomes coarser (i.e., at lower bit rates). Intuitively, both hardware fault and quantization contribute to additional distortion in the decoded images, but as quantization quantization distortion increases the additional distortion due to the fault becomes negligible.

Bit/R	1	4	8
0	-0.0030	-0.0009	0.0008
1	-0.0056	-0.0007	0.0002
2	-0.0154	-0.0022	-0.0009
3	-0.0489	-0.0083	-0.0008
4	-0.1943	-0.0257	-0.0082
5	*-0.6406*	-0.1066	-0.0293
6	*-2.6987*	*-0.4066*	-0.1308
7	*-5.3202*	*-1.8567*	*-0.3713*

Table 1. Changes in decoded image quality due to a SSF at the input of DCT. The quality change is measured for a test image by computing the difference in the PSNR of the decoded image obtained from a fault-free JPEG encoder and that produced by a faulty JPEG encoder. A negative value corresponds quality degradation. Bit 0 corresponds to the least significant bit of an input pixel. The parameter R controls the quantization level, with larger R corresponding to coarser quantization (i.e., lower bit-rate and worse decoded image quality.)

Our goal is to define a methodology to discriminate between acceptable and unacceptable faults in systems comprised of a linear transform followed by quantization. To do so, we propose tools to (i) estimate the effect of individual faults at the system output, and (ii) decide on thresholds of acceptable degradation, which will be used to determine whether each specific fault is acceptable or not. This will require analyzing specific system architectures and also taking into account the characteristics of the input (i.e., the statistics of typical image data), as well as specific image/video quality requirements in the application. With this methodology we then seek to generate testing methods to classify systems with unknown faults into acceptable and unacceptable systems. As compared to previous work on testing for ET [7], a significant novelty in this paper is that we consider typical input statistics, instead of assuming a simple uniform distribution of inputs [7]. We also propose novel application-specific error rate testing techniques. Our results are specific to the analysis of linear transforms followed by quantization, and our acceptable degradation thresholds take into account the perceptual effect of faults on typical image and video compression applications.

Our results show that a significant fraction (e.g., over 50% in some cases) of interconnection faults within a 1D DCT module are acceptable in a JPEG encoder (operating at any of its admissible compression rates). Our acceptability criteria take into account the maximum error produced at the output (the error is dependent on the input), as well as the rate at which errors of a given magnitude occur. We also propose techniques to reduce the number of test vectors to be used, and show that a small number of test vectors leads to practically the same test coverage (the difference is within 1%, with a a factor of 64 reduction in the number of test vectors.)

The paper is organized as follows. In Section 2, we propose a general framework for analyzing linear

---

[1]Quality differences as high as 0.5dB are often difficult to perceive in typical image and video coding applications. As we will see later in this paper the errors introduced due to faults are different from typical errors introduced by lossy compression and thus we will need to take into account both maximum error and probability of error measurements.

transforms followed by quantization and provide tools to quantify the effect of faults at the output. In Section 3, we use the DCT as an example and propose a method to select perceptual error thresholds. We also present an overview of fault analysis method. Finally, in Section 4, we propose heuristic methods to reduce the size of the set of test vectors, while preserving the accuracy of our estimates of the error statistics. We provide results to illustrate the performance of these test vectors for testing a 1D DCT module.

2. System level fault tolerance in linear transform and quantization

Invertible linear transforms are used to extract meaningful frequency information from signals. In lossy compression applications these transforms are followed by quantization, as shown in Figure 1. The input to the system is a vector $\bar{\mathbf{X}}$, which we assume drawn from a vector distribution that can be statistically characterized, e.g., by its covariance structure. We can define the set of possible faults, or fault space, $\mathbf{F}$, by analyzing the architecture of the system. Assume there is a single fault $f_i \in \mathbf{F}$ in the transform and denote its faulty (vector) output $\bar{\mathbf{Y}}'$. Denote $\bar{\mathbf{Y}}$ the output of the fault-free system when the input is $\bar{\mathbf{X}}$. Our goal is
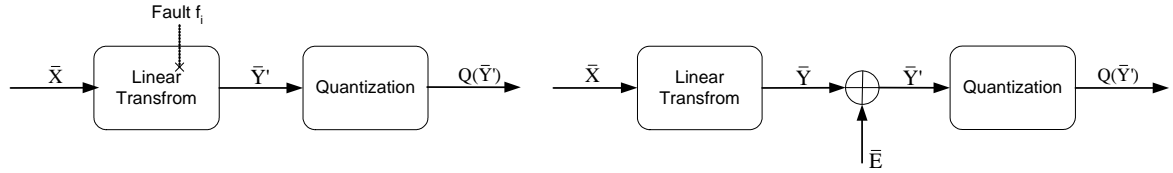

Figure 1. Linear Transform and Quantization

to analyze whether a particular fault f_i is acceptable. To simplify the analysis we view the effect of the fault as a term $\bar{\mathbf{E}}$ added to the fault-free output $\bar{\mathbf{Y}}$. Clearly, $\bar{\mathbf{E}}$ is a deterministic function of f_i, $\bar{\mathbf{X}}$, and the structure of the linear transform. Since we consider invertible transforms, there is a 1-to-1 mapping between $\bar{\mathbf{X}}$ and $\bar{\mathbf{Y}}$, and thus, $\bar{\mathbf{E}}$ is not independent of $\bar{\mathbf{Y}}$.

2.1. Quantization Analysis

Note that scalar quantization is normally used, so that each component of $\bar{\mathbf{Y}}$ (or $\bar{\mathbf{Y}}'$) is independently quantized. Denote Y_i, E_i, Y_i' the i-th component of the vectors $\bar{\mathbf{Y}}$, $\bar{\mathbf{E}}$, and $\bar{\mathbf{Y}}'$, respectively, with $i = 1 \ldots N$, and N the vector dimension. When considering individual components it is reasonable to assume that E_i will be independent of Y_i, even though $\bar{\mathbf{Y}}$ and $\bar{\mathbf{E}}$ are dependent. To see why, note that for a specific value of Y_i there are many possible values of E_i, which depend on the Y_j, $j \neq i$. In what follows we make the assumption that E_i is a random additive error term independent of Y_i. We have verified that this is a reasonable assumption for typical systems. For convenience, in what follows we focus on one component and drop the subscript i.

Our focus now turns to analyzing how the error E leads to additional error *after quantization* (refer to Figure 2). Let E and Y be discrete and continuous random variables, respectively, with known pmf/pdf. We use absolute difference as a distortion metric, due to its computational simplicity. Let the quantization bin size be Δ and define $\Delta D = D_{QE} - D_Q$, the additional distortion after quantization due to the error E, where $D_{QE} = |Q(Y') - Y|$ is the distortion due to both quantization and error, and $D_Q = |Q(Y) - Y|$ is the distortion due only to quantization.
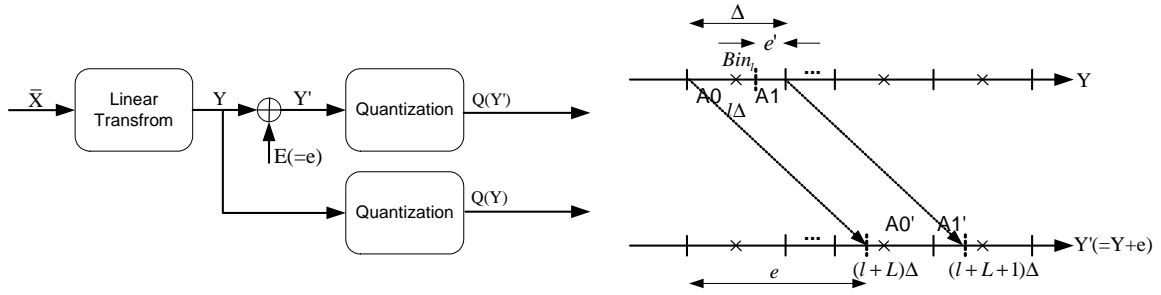
To facilitate the analysis, we will represent E as follows:

$$E = L\Delta + E',$$

where $L = \lfloor \frac{E}{\Delta} \rfloor$ is a non-negative integer and $0 \leq E' < \Delta$.

Figure 2 illustrates the relationship between $Q(Y')$ and $Q(Y)$. As can be seen in the figure, for $Q(Y) = l\Delta$, and for a given error, $Q(Y')$ can take two different values, depending on the original value of Y. More formally (refer to Fig. 2):

$$Q(Y') = \begin{cases} (l + L + 1)\Delta, & if \ Y \ \in \ \mathbf{A1} \\ (l + L)\Delta, & if \ Y \ \in \ \mathbf{A0} \end{cases} \tag{1}$$

Figure 2. Quantization Analysis. Y **is quantized into bins of size** (Δ). **If we focus on one bin** (Bin_l), $Q(Y) = l\Delta$ **is the center of that bin.** $Y' = Y + e$ **now belongs to a different quantization bin. There are two cases for a given error** e. **If** $Y' \in \mathbf{A1}'$ **then** $Q(Y') \in (l+L+1)\Delta$. **Alternatively,** $Y' \in \mathbf{A0}'$, **corresponding to** $Y \in \mathbf{A0}$, **leads to** $Q(Y') \in (l+L)\Delta$. **Thus two errors are possible when** $Y \in Bin_l$.

We now use (1) to evaluate the error added at the output due to the fault. Mean square error (MSE) is the most popular objective distortion metric for image and video coding applications. However, we argue that MSE *is not* a suitable choice for our problem. In a typical compression scenario quantization is designed so that quantization noise affects all components of $\bar{\mathbf{Y}}$ in a controlled manner, according to perceptual criteria. Instead, we are now considering error produced by a fault, which has no such properties, and thus can be unevenly distributed over the various components of $\bar{\mathbf{Y}}$. In our evaluation this is indeed the case: for example, certain faults produce no errors at the output for most image blocks and very visible errors for a few blocks. In this situation MSE would not a suitable metric, since a large error in a few blocks, while clearly visible by the end user, could still lead to a low overall MSE. As an alternative we propose (i) a maximum error metric (E_{max}), which measures the worst possible additional error after quantization (for any input), and ii) an error rate (P_o) metric, measuring the probability that unacceptable degradation occurs for a given input pdf.

2.1.1. E_{max} and P_o analysis
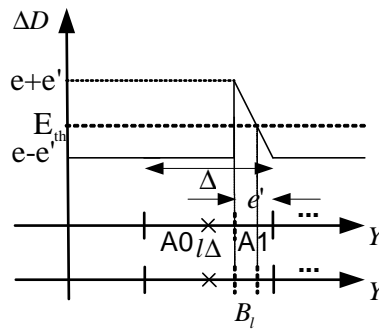
Figure 3. Relation between ΔD **and Y. At the edge of** $A1$ ΔD **has maximum.** $\mathbf{B_i}$ **is the range of** Y **in each quantization bin** (Bin_i) **where** ΔD **is larger than error threshold (**E_{th}**). We need to integrate** $f_Y(y)$ **over this range to get error rate.**

Figure 3 depicts the relationship between ΔD and Y for a particular value of the error e, and with $e = L \cdot \Delta + e'$. Consider first the situation where $L = 0$, i.e., $e < \Delta$ and $e' = e$, and observe two different cases. First, if $Y \in A1 = [(l+0.5)\Delta - e', (l+0.5)\Delta]$, then $\Delta D = |(l+1)\Delta - Y| - |l\Delta - Y|$ (because the error due to the fault shifts the input to the quantizer enough to move the output to the next quantization bin.) In this case, as Y increases, $|l\Delta - Y|$ increases, $|(l+1)\Delta - Y|$ decreases, and thus ΔD decreases. Instead if $Y \in A0 = [(l-0.5)\Delta, (l+0.5)\Delta - e']$, $\Delta D = |l\Delta - Y| - |l\Delta - Y| = 0$. Similar results can be obtained when L is non-zero, by adding $L\Delta$ to the final error (for inputs in both intervals $A0$ and $A1$). From Figure 3, we see that $E_{max} = E + E'$ (when $E \le \Delta$, $E_{max} = 2E$, since $E = E'$). To determine P_o, we first select

an error threshold for acceptable degradation, which we denote E_{th}. Then we define P_o as follows:

$$P_o = \sum_e P(\Delta D \geq E_{th}|E = e)P_E(e). \tag{2}$$

$P(\Delta D \geq E_{th}|E = e)$ has different expressions depending on the relative values of error (e) and error threshold (E_{th}).

$$P(\Delta D \geq E_{th}|E = e) = \begin{cases} \int_{\bigcup \mathbf{B_i}} f_Y(y)dy, e - e' < Eth < e + e' \\ 0, E_{th} > e + e' \\ 1, E_{th} < e - e' \end{cases} \tag{3}$$

$$\mathbf{B_i} = \{Y| \ i\Delta + \tfrac{\Delta}{2} - e' \leqq Y < i\Delta + \tfrac{\Delta}{2} - e' + \tfrac{e+e'-E_{th}}{2}\}$$

Here $\mathbf{B_i}$ is the range of Y in each quantization bin (Bin_i) where $\Delta D \geq E_{th}$. Then using (3), we can write:

$$P_o = \sum_{\frac{E_{th}}{\Delta} - \frac{2e'}{\Delta} < \lfloor \frac{e}{\Delta} \rfloor < \frac{E_{th}}{\Delta}} P_E(e) \int_{\bigcup \mathbf{B_i}} f_Y(y)dy + \sum_{\lfloor \frac{e}{\Delta} \rfloor > \frac{E_{th}}{\Delta}} P_E(e) \tag{4}$$

To simplify (4), we assume that the pdf of Y ($f_Y(y)$) is smooth, and we define K as follows:

$$K = \frac{\int_{\bigcup \mathbf{B_i}} f_Y(y)dy}{|B_i|/\Delta}, |B_i| : e + e' - E_{th}(interval \ of \ B_i) \tag{5}$$

where, depending on the relative values of σ_{max} and Δ, K can be written as follows:

- Case 1: $K \approx 1, \Delta << \sigma_{max}$
- Case 2: $K < 1, \Delta = G\sigma_{max}, (G \approx 1)$
- Case 3: $K \approx 0, \Delta >> \sigma_{max}$

Thus, when the quantization bin size is much smaller than the dynamic range of the signal, as characterized by σ_{max}, i.e. in Case 1, from (5) $\int_{\bigcup \mathbf{B_i}} f_Y(y)dy \simeq |B_i|/\Delta$. As Δ becomes smaller relative to σ_{max} (Cases 2 and 3), $\int_{\bigcup \mathbf{B_i}} f_Y(y)dy$ decreases. We can then write P_o as a function of K as:

$$P_o = \sum_{\frac{E_{th}}{\Delta} - \frac{2e'}{\Delta} < \lfloor \frac{e}{\Delta} \rfloor < \frac{E_{th}}{\Delta}} P_E(e)K\frac{e + e' - E_{th}}{2\Delta} + \sum_{\lfloor \frac{e}{\Delta} \rfloor > \frac{E_{th}}{\Delta}} P_E(e) \tag{6}$$

As can be seen in (6), in order to estimate P_o, we need to select a threshold and estimate the pdf/pmf of Y and E. This is addressed in the next section.

3. System level fault tolerance in DCT and quantization

We now provide a more detailed analysis of the transform operation, using the Discrete Cosine Transform (DCT) as an example. Figure 4 shows the basic structure of a 2D separable DCT system [11], which can be implemented using two 1D DCT systems and some memory. Note that the 1D DCT is composed of parallel PE_i modules, where each processing element calculates the dot product between input vector $\bar{\mathbf{X}}$ and one of the 1D DCT basis vectors $\bar{\mathbf{C_i}}$, which will be denoted DC (lowest frequency) and $AC1$ to $AC7$ (with $AC7$ being the highest frequency basis vector).

3.1. Problem formulation

The input ($X(i,j)$) to the 2D DCT is an $N \times N$ block of image pixels and the output ($Y(u,v)$) is a matrix of size $N \times N$, where each entry represents a frequency component of the original image block. Each of these "frequency coefficients" is quantized independently, and $E(u,v)$ is assumed independent of $Y(u,v)$ as discussed in the previous section. Among the various structures proposed for PE_i [11], we select a simple serial multiplication and accumulation structure shown in Figure 4. The fault space $\mathbf{F}$ is assumed to include only single stuck-at faults (SSF) on interconnections. We assume that the pdf of $Y(u,v)$ is known based on statistics gathered from typical images.
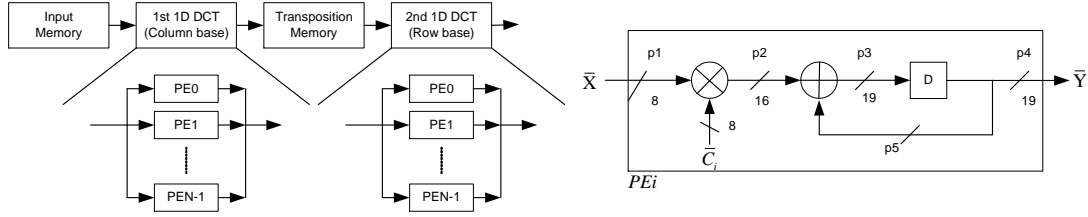
Figure 4. DCT block diagram

3.2. Metric and System Analysis

Our design will be based on setting thresholds for a maximum error value for each frequency, $E_{th}(u,v)$, and a threshold P_{th} for the probability of exceeding that error (their selection will be discussed in Section 3.3). The expression derived in Section 2.1.1 allowed us to calculate P_o for one frequency component. Now we need to combine these individual values ($P_o(u,v)$) into a global P_o; this can be done using the summation law:

$$P_o = 1 - \prod_{u=1}^{N} \prod_{v=1}^{N} (1 - P_o(u,v)). \tag{7}$$

If we assume $P_o(u,v)$ is small for all u,v, then $P_o \approx \sum_{u=1}^{N} \sum_{v=1}^{N} P_o(u,v)$. Therefore, for a fault to be acceptable with a given probability of error threshold P_{th}, the following will have to hold:

$$\sum_{u=1}^{N} \sum_{v=1}^{N} P_o(u,v) \le P_{th}. \tag{8}$$

Using the above metrics, we now summarize our analysis of the DCT system. First, we perform a *error analysis* to obtain for each possible fault a random variable ($E(u,v)$) that captures the error added by the fault. This will allows us to compute P_o and E_{max}, using the input statistics and any chosen error threshold (E_{th}). Second, we perform a *threshold analysis* to determine appropriate error threshold ($E_{th}(u,v)$) and error rate threshold (P_{th}) for the application (as will be discussed in next section.) With this information, we can proceed to the *fault analysis*, to determine whether a specific fault is acceptable or not. In the fault analysis, $E(u,v)$ depends on the DCT structure, input pdf, and fault f_i, and we can get statistics of $E(u,v)$ by simulation, analysis of the system, or using a set of test vectors.

3.3. Perceptual threshold

In our analysis, we have two types of thresholds. First, an error threshold ($E_{th}(u,v)$) for each frequency component is selected using perceptual thresholds derived from human visual system criteria [3], [10]. For example, in [3], a perceptual threshold is obtained for each DCT coefficient which is used to determine what constitutes perceptually lossless quantization for each coefficient. If the error in one coefficient of DCT basis exceeds threshold value, then perceptible distortion can be found in the output in the form of a DCT basis pattern (regular pattern in pixel domain). Due to variations in the contrast sensitivity of the human visual system as a function of spatial frequency, different thresholds are selected at different frequencies. Note that in our case we are concerned with the perceptual difference between *two quantized images*, rather than a quantized image and an original one, as in [3]. This is important because we have observed that as quantization becomes coarser, the effect of errors becomes less significant. Roughly speaking, when quantization is very coarse, even large errors due to faults will not lead to changes in the quantized output (i.e., the original value and the one with error added are quantized to the same bin.)

This allows us to use a bigger threshold than the original perceptual threshold ($E_{th,orig}$) in the case of coefficients with small dynamic range (σ_{max}), as compared to the quantization step size (Δ). To take advantage of this we use a heuristic modification of the threshold. We assume that errors that are less than $\Delta - \sigma_{max}$ will typically not lead to changes in the quantized data (here σ_{max} is an estimate of the dynamic range of the signal). Then we replace the original perceptual threshold by $E_{th}(u,v) = max(E_{th,orig}, \Delta - \sigma_{max})$ in Case 3 of Section 2.1. For Case 1 and Case 2, $E_{th}(u,v) = E_{th,orig}$, i.e., we use the same threshold

as in [3]. The second threshold to select is the application-specific error rate threshold P_{th}. If the application has strict quality constraints, then a low P_{th} will have to be chosen. We provide some example images with various P_{th} values in [1].

3.4. Fault Analysis

Using the above analysis, we propose a fault analysis algorithm, depicted in Figure 5. Basically our analysis consists of two stages. First, error significance analysis determines whether the maximum error value is bigger than an error threshold for each frequency component. If the maximum error is smaller than the threshold for all frequencies, then faults in the system are acceptable. Note that a testing method has been developed in [7] using this type of analysis for cases when inputs are uniformly distributed. The whole input space is searched, and at least one test vector is found for each detectable fault in fault space $\mathbf{F}$. So the number of test vectors is almost the same as the number of faults in $\mathbf{F}$. In our work, however, we are considering a specific input pdf, which captures typical image characteristics and thus we need an alternative testing method.

The second stage is the error rate analysis, which checks how often unacceptable errors occur due to a fault in the system, based on pmf/pdf of E and Y. The pdf of Y is given, but the pmf of E is not, and would be obtained via testing. Our goal is to obtain the pmf of E using small number of test vectors. This is addressed in the next section.
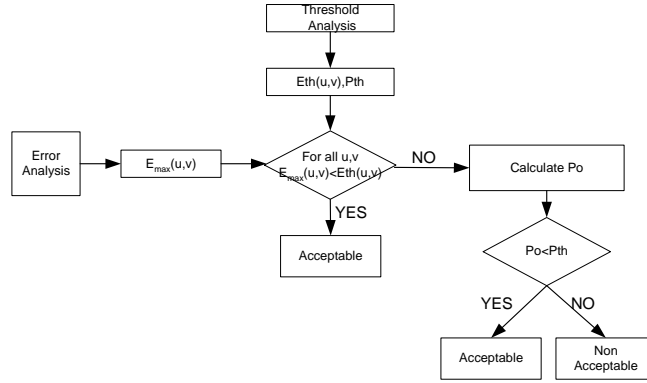

Figure 5. Overview of Fault Analsis

4. System Level Fault Testing

4.1. Problem formulation

Denote the vector input to the system $\bar{\mathbf{X}}$. Assume we have access to both a faulty and a fault-free system. The error can be computed by subtracting the output of the faulty system from the output of fault free system. Assume we start with an initial set of test vectors ($\mathbf{I}$), large enough to provide an arbitrarily good approximation to the pmf of E ($P_E(e)$). We would like to select a smaller set ($\mathbf{S}$) which generates estimated pmf of E ($P_{E,sub}(e)$). N_I and N_S are the sizes of $\mathbf{I}$ and $\mathbf{S}$, respectively. Our goal is to reduce the number of input in set $\mathbf{I}$ such that $P_{E,sub}(e)$ is similar to $P_E(e)$ for for all faults in fault space $\mathbf{F}$. As similarity metric between the two pmfs we use the correlation between the two pmfs:

$$Corr(P_E(e), P_{E,sub}(e)) = \frac{\sum P_E(e)P_{E,sub}(e)}{\sqrt{\sum P_E(e)^2 \sum P_{E,sub}(e)^2}} \tag{9}$$

4.2. Heuristic Solutions and Results

A 2D DCT system is implemented using two 1D DCT systems, with each 1D DCT composed of N PE_is. Here we assume all PE_i in the 1st 1D DCT have the structure shown in Figure 4. Dimension of DCT (N) is 8, and the fault space $\mathbf{F}$ consists of SSF in interconnections represented by p1~p5 of PE_i. $\bar{\mathbf{C}}_{\mathbf{i}}$ will be one

of the 8 1D DCT basis vectors (from DC to $AC7$) depending on the specific PE_i considered. We will be selecting test vectors that can be used to test all PE's. As initial set (**I**), we used a typical test image, which is decomposed into 1×8 vectors. We tried three types of reduced input set (**S**) which have the same number of test vectors (N_S).

Method 1: Assume each frequency component to be Gaussian, and calculate mean and variance of each frequency component using initial set (**I**).Then use random Gaussian generator with those parameters. (**S₁**)

Method 2: Downsize initial set image using filtering and down sampling. Then use that small size image to get test vectors. (**S₂**)

Method 3: Using 1×8 vectors from initial set, regularly subsample those 1D vectors. (**S₃**)

(a) Method 1   (b) Method 2   (c) Method 3
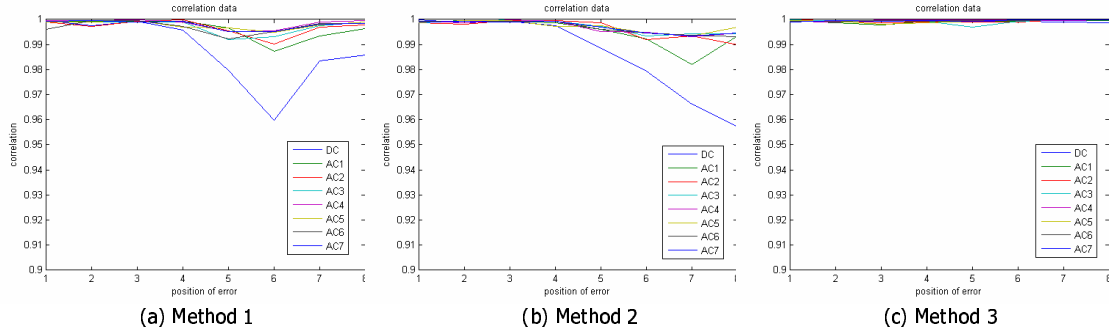
Figure 6. Testing Performance of Reduced Vector Set using Correlation metric

Figure 6 shows the correlation between the actual and estimated pmfs when we insert a fault in each interconnection line of $p1$ position of PE_i block. X axis in Figure 6 represents position of faults (LSB to MSB) in each interconnection and each line represents each basis . As can be seen in Figure 6, *Method 3* shows the best performance among three methods (with the subset size $\frac{1}{64}$ of initial one) and this method also shows the best performance in case of other fault positions in $p2$, $p3$, $p4$, and $p5$ cases. The correlation between two pmfs is always over 0.99 in all cases.

Now we test the first 1D DCT module (column-wise DCT) in the 2D DCT system in Figure 4 using the above reduced test vector set (**S₃**) to test both error significance and error rate. Recall that our error threshold values ($E_{th}(u, v)$) are for the 2D DCT system. Thus, we need to translate these into thresholds applicable to the first 1D DCT system.

Assume that there is a SSF (f_k) in one specific PE_i of the first (column-wise) 1D DCT module. When we perform a series of 1D DCTs for each column of an input 8×8 image block, a series of errors is generated by f_k in PE_i module, and those errors are stored in the i_{th} of each 8×8 output block stored in the transposition memory. We observe that these errors are strongly correlated if f_k occurs in higher bit positions and weakly correlated if it occurs in lower bit positions within one 8×8 image block.

After the second (row-wise) 1D DCT, for higher bit cases, due to correlation, the final error in the 2D DCT output is concentrated on the first column of the i_{th}, i.e., $E(i, 1)$ will contain most of the error energy. For lower bit cases, due to the lack of correlation, error will be spread over all columns of the i_{th} row, i.e., $E(i, 1) \sim E(i, 8)$ will all contain relative similar amounts of energy. To simplify we assume that errors are also highly correlated in lower bit cases, which is clearly a worse case scenario than assuming evenly spread errors. Under this assumption, we can have a lower bound for the percentage of acceptable faults. Thus when E is the error produced by PE_i, the final error $E(i, 1)$ in the 2D DCT output will $\sqrt{N}E$ because 1D DC basis is $[\frac{1}{\sqrt{N}}, ..., \frac{1}{\sqrt{N}}]$ and $\frac{1}{\sqrt{N}} \times N \times E = \sqrt{N}E$. Using the above assumption, given $E_{th}(1, i)$, we can select the acceptability threshold for the first 1D DCT as $E_{th,1D}(i) = \frac{E_{th}(1,i)}{\sqrt{N}}$, which ensures that acceptable faults (in the first 1D DCT) result in images that are perceptually lossless.

In our experiments we change the error rate threshold value (P_{th}) and the quantization bin size to observe relation between those parameters and percentage of acceptable faults. The quantization bin size is modified by multiplying an integer Q_p value to the basic JPEG quantization table.

Figure 7 shows percentage of acceptable faults using initial set (**I**) and reduced set (**S**). The difference
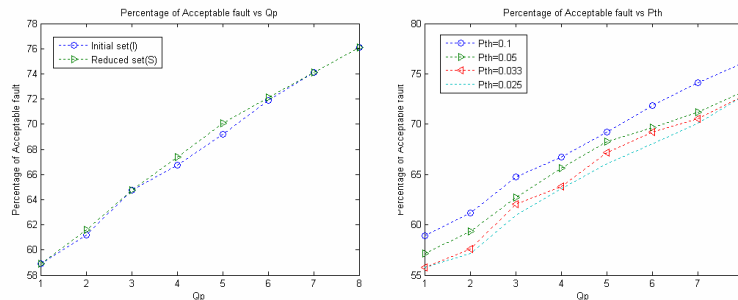
Figure 7. Testing Performance of S_3 for 1D DCT block

between the two cases is relatively small. So we can test the first 1D DCT system using **S** with enough confidence. Also we can observe that the percentage of acceptable faults is over 50% in all operating range, and as quantization bin sizes increase, so does the percentage of acceptable faults. This is because as quantization bin size increases, more quantization noise occurs, which makes the system more resilient to larger errors due to faults. Another observation is that as error rate threshold increases, more faults are acceptable, because we loosen the standard for acceptable degradation.

5. Conclusion

We presented a general framework for analyzing linear transform followed by quantization. We estimated faults' impact on the system, by analyzing quantization block and linear transform block separately. Faults in the linear transform are modeled as errors added to the output of transform. More specifically we chose the DCT as a transform of interest, and introduced perceptual thresholds for acceptable degradation, which enables categorizing chips into acceptable and unacceptable. Using these perceptual thresholds and our system analysis, we proposed a general fault analysis for this system which consists of error significance and error rate analysis. The error pmf is estimated using a small number of test vectors to minimize test costs. Our results show that a significant fraction (e.g., over 50% in some cases) of interconnection faults within a first 1D DCT module are acceptable in a JPEG encoder operating at any of its available compression rates.

References

[1] http://biron.usc.edu/wiki/index.php/ETComp.

[2] Draft ITU-T recommendation and final draft international standard of joint video specification (ITU-T Rec. H.264/ISO/IEC 14 496-10 AVC in Joint Video Team(JVT) of ISO/IEC MPEG and ITU-T VCEG, JVT-G050, 2003.

[3] A. J. J. Ahumada and A. Watson. An improved detection model for DCT coefficient quantization. In *Human Vision, Visual Processing, and Digital Display IV. Allebach ed., SPIE*, 1993.

[4] M. A. Breuer, S. K. Gupta, and T. M. Mak. Defect and error tolerance in the presence of massive numbers of defects. *IEEE Design & Test of Computers*, 21:216–227, May–June 2004.

[5] H. Chung and A. Ortega. System level fault tolerance for motion estimation. Technical Report USC-SIPI354, Signal and Image Processing Institute, Univ. of Southern California, 2002.

[6] H. Chung and A. Ortega. Analysis and testing for error tolerant motion estimation. In *Proc. of IEEE International Symposium on Defect and Fault Tolerance in VLSI Systems, DFT'05*, Monterey, CA, Oct. 2005.

[7] Z. Jiang and S. Gupta. An ATPG for threshold testing: Obtaining acceptable yield in future processes. In *International Test Conference*, 2002.

[8] J. L. Mitchell and W. B. Pennebaker. *JPEG Still image data compression standard*. Van Nostrand Reinhold, New York, 1993.

[9] J. L. Mitchell, W. B. Pennebaker, C. E. Fogg, and D. J. LeGall. *MPEG Video Compression Standard*. Chapman and Hall, New York, 1997.

[10] H. A. Peterson, H. Peng, J. H. Morgan, and W. B. Pennebaker. Quantization of color image components in the DCT domain. In *Human Vision, Visual Processing, and Digital Display II., SPIE*, volume 1453, 1991.

[11] K. R. Rao and P. Yip. *Discrete Cosine Transform*. Academic Press, United States, 1990.

[12] K. Sayood. *Introduction to Data Compression*. Morgan Kaufman, United States, 2000.